

Nonlinear NMR in a Superfluid ^3He B-Like Phase in Aerogel

V. V. Dmitriev^{1,*}, V. V. Zav'yalov¹, D. E. Zmeev¹, I. V. Kosarev¹, and N. Mulders²

¹ Kapitza Institute of Physical Problems, Russian Academy of Sciences, Moscow, 119334 Russia

* e-mail: dmitriev@kapitza.ras.ru

² Department of Physics and Astronomy, University of Delaware, Newark, Delaware 19716, USA

Received August 1, 2002

The properties of liquid ^3He in a low-density aerogel preliminarily covered with a few monolayers of ^4He were studied by pulsed and nonlinear continuous NMR techniques. It was found that a NMR frequency shift from the Larmor value exhibits a sharp increase at a magnetization rotation angle exceeding 104° . Nonlinear continuous NMR signals related to the formation of a macroscopic region featuring homogeneous precession of the magnetization (homogeneous precession domain) were observed. The experimental results confirm that the low-temperature superfluid ^3He phase in the aerogel is analogous to the B-phase in bulk ^3He and indicate that the superfluid spin currents play an important role in the spin dynamics of superfluid ^3He in aerogel. © 2002 MAIK "Nauka/Interperiodica".

PACS numbers: 67.57.Lm; 76.60.-k

1. INTRODUCTION

The theory of superfluid ^3He phases is well developed and in most cases shows a quantitative agreement with experiment. For this reason, superfluid ^3He is an ideal object for verification of the theoretical models of systems with nontrivial Cooper spin pairing. Presently, an important problem is to study the influence of impurities on such objects. Such a possibility was offered by development of the technology of low-density aerogels. An aerogel represents a "mop" consisting of SiO_2 fibers with a diameter on the order of 30 \AA , while a characteristic distance between fibers amounts to $500\text{--}1000 \text{ \AA}$ (we imply the so-called 98% aerogel, in which 98% of the volume is free, employed in most experiments with ^3He). Since the coherence length of superfluid ^3He (amounting to several hundreds of Angströms) significantly exceeds the diameter of fibers, the fibers play the role of impurities in ^3He .

The superfluidity of ^3He in aerogel was discovered several years ago [1, 2]. At present, it is known that the presence of fibers leads to a small (20–30%) depression of the superfluid transition temperature in ^3He and that two superfluid ^3He phases, analogous to the superfluid A and B phases in bulk ^3He , may exist in the aerogel [3, 4]. However, the phase diagram of superfluid ^3He in aerogel exhibits qualitative differences from that of bulk ^3He . In particular, the region of existence of the equilibrium A-like phase is much smaller (even at large pressures and in strong magnetic fields) as compared to that of bulk ^3He ; however, the A-like phase remains stable in a sufficiently wide temperature interval in a supercooled state.

Experiments in aerogel can be performed both with pure ^3He and in the presence of a small admixture of ^4He . In the former case, the NMR spectrum is significantly influenced by the paramagnetic solid ^3He possessing a high magnetic susceptibility at low temperatures, two monolayers of which cover the surface of fibers. Upon the introduction of ^4He , solid ^3He is replaced by nonmagnetic ^4He and the NMR response is fully determined by the liquid ^3He .

2. NMR in bulk ^3He -B. In the superfluid B phase of bulk ^3He , the frequency of linear (at small excitation amplitudes) continuous NMR is determined by the angle ψ between the direction of external magnetic field \mathbf{H} and the order parameter vector \mathbf{n} : $\omega \approx \omega_L + \frac{\Omega_B^2}{2\omega_L} \sin^2\psi$, where Ω_B is the temperature-dependent longitudinal resonance frequency (Leggett frequency) for ^3He -B and $\omega_L = \gamma H$ is the Larmor frequency. Far from the cell walls, $\mathbf{n} \parallel \mathbf{H}$ and $\omega = \omega_L$. Near the wall, $\psi \approx 63^\circ$ for \mathbf{H} parallel to the wall plane, which leads to a shift of the frequency. As a result, the absorption line in the linear continuous NMR spectrum become asymmetric, comprising a peak at the Larmor frequency and a long "tail" extended toward high frequencies and determined by a spatial distribution (texture) of the order parameter.

In the case of a pulsed NMR measured for sufficiently large magnetization rotation angles β , the system exhibits a texture transition and the \mathbf{M} and \mathbf{n} vectors exhibit precession as if the walls were absent (the Brinkman–Smith mode) [5]. The frequency of precession is ω_L if the β value does not exceed $\Theta_0 =$

$\arccos(-1/4) \approx 104^\circ$. For $\beta > \Theta_0$, the precession frequency varies by the law

$$\omega = \omega_L - \frac{4\Omega_B^2}{5\omega_L}(1 + 4\cos\beta)$$

The presence of spatial inhomogeneities of the precessing magnetization (e.g., due to a gradient of the field H) leads to the appearance of superfluid spin currents (spin supercurrents) carrying the longitudinal magnetization component. As a result, a homogeneously precessing two-domain structure (homogeneous precession domain, HPD [6]) may form in a closed ^3He -B volume. One of these domains represents a region of virtually equilibrium magnetization; in the other, the magnetization vector is rotated by an angle close to Θ_0 and exhibits in-phase precession at a Larmor frequency at the interdomain boundary, a characteristic thickness of which usually amounts to 0.2–0.3 mm. The spin supercurrents also play an important role in determining the stability of an HPD: spatial inhomogeneities give rise to currents which tend to restore homogeneous precession.

Under continuous NMR conditions, when a homogeneous magnetic field gradient (parallel to \mathbf{H} and directed in the z axis) is applied to a sample and the RF field frequency ω_f is fixed, an HPD is formed in the course of a gradual decrease of the homogeneous component of the external magnetic field H_0 (the RF field amplitude must be sufficiently large) [7]. The HPD begins to form when the coordinate z (determined by the condition $\omega_f = \gamma H(z)$) reaches the cell boundary (z_c). Owing to the spin supercurrents, the magnetization rotation angle in this region may reach and even exceed the Θ_0 value. When the field H_0 decreases, this region of the cell keeps in resonance with the RF field (due to the fact that β slightly exceeds Θ_0), which leads to a positive frequency shift. As a result, the HPD size increases and the spatial distribution of β is determined by the condition that the frequency of precession is equal to that of the RF field; the domain wall coordinate is determined by the resonance condition $\omega_f = \gamma H(z_0)$. The absorbed RF power is determined by a phase difference between the precessing magnetization and the RF field. This difference is established on a level such that the absorbed power equals the power dissipated within the HPD via the magnetic relaxation processes. The dissipation increases with the HPD size. As the H_0 keeps decreasing, the HPD breaks (and does not restore when H_0 is scanned in the reverse direction). If the RF field is switched off in the presence of an HPD, the domain will retain its homogeneity and the magnetic relaxation will only reduce the HPD size: the domain boundary keeps moving and the frequency of a long-lived induction signal (the duration of which is significantly greater than the characteristic time of dephasing in an inhomogeneous magnetic field: $\tau = (\gamma\sqrt{H}L)^{-1}$,

where L is the cell length) gradually decreases from ω_f to $\gamma H(z_c)$.

If the order parameter of a low-temperature superfluid ^3He phase in aerogel corresponds to that of the B phase in bulk ^3He , the NMR behavior in this system must be similar to those observed in bulk ^3He -B. Accordingly, it is natural to expect that the dependence of ω on β for nonlinear NMR would exhibit a feature at $\beta \approx 104^\circ$. It can be also suggested that the spin supercurrents in ^3He B-like phase in aerogel are qualitatively similar to those in bulk ^3He -B and can lead to the HPD formation. However, until now the NMR investigations of ^3He in aerogel were mostly restricted to linear continuous NMR response. These experiments showed that the NMR behavior of ^3He B-like phase in aerogel is in fact like that of bulk ^3He -B: the NMR line exhibits broadening toward high frequencies (while a quantity analogous to the Leggett frequency is several times smaller in aerogel than in bulk ^3He -B) and the decay of magnetic susceptibility with decreasing temperature is similar to that observed in bulk ^3He -B.

To the present, the pulsed NMR measurements were performed either for the pure ^3He in aerogel (whereat no features in dependence of the NMR frequency on β were found near $\beta \approx \Theta_0$) or at small magnetization rotation angles [2, 8]. Recently, a study of the nonlinear continuous NMR in superfluid ^3He B-like phase in aerogel was reported by the Grenoble group [[9]. The NMR signal characteristics (dependence on the scan direction and the field gradient) reported in [9] corresponded to the behavior typical of the HPD. However, the region of existence and the amplitude of the signal observed in [9] were smaller than one may expect from an HPD with the length significantly exceeding the domain wall thickness. Thus, the question concerning the possible HPD formation in the B-like phase of ^3He in aerogel did not receive unambiguous answer.

The aim of our experiments was to study the nonlinear NMR (in both pulsed and continuous modes) in superfluid B-like phase of ^3He in aerogel. The experiments were conducted in an aerogel with the surface covered with two monolayers (calculated estimate) of ^4He .

3. Experimental. The experiments were performed at a pressure of 25.5 bar in a magnetic field varied from 284 to 1082 Oe (which corresponded to the NMR frequencies from 922 kHz to 3.51 MHz). The experimental chamber (Fig.1), mounted on a nuclear demagnetization stage, comprised two like cells of the same cylindrical shape (diameter, 5.3 mm; height, 5.6 mm) made of a Stycast-1266 epoxy resin. Each cell was surrounded by NMR coils (thermally insulated from the cell body). The first cell (cell 1) was almost completely filled with a 98% aerogel (except for 0.15 mm gaps between aerogel and internal wall surface). The second cell (cell 2) contained aerogel in the form of a disk with a thickness of ~ 2.4 mm, which was situated in the mid-

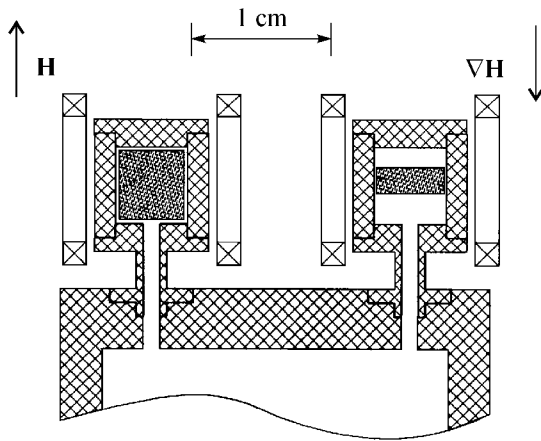


Fig. 1. Schematic diagram of the experimental chamber (see the text for explanations).

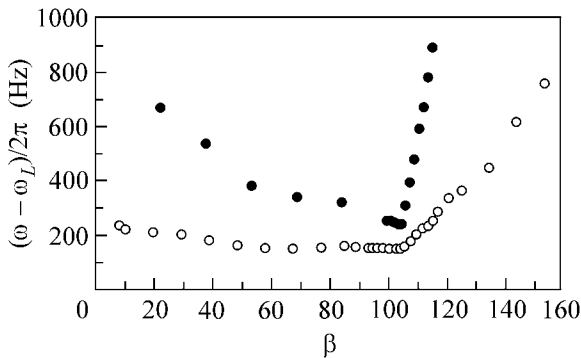


Fig. 2. Plots of the induction signal onset frequency versus magnetization rotation angle for ^3He B-like phase in aerogel measured at (1) $H = 1.01$ kOe, $T \approx 0.83 T_c^a$ and (2) $H = 285$ Oe, $T \approx 0.78 T_c^a$.

dle part of the sample volume. The required temperature was provided by a nuclear demagnetization cryostat and monitored by a platinum NMR thermometer gauge located in a special volume below the experimental cells.

4. Pulsed NMR of ^3He -B in aerogel. The pulsed NMR measurements were conducted only with cell 1. The sample was exposed to magnetization-rotating RF pulses at the NMR probe frequency. The free precession (induction) response signals were recorded in a computer memory and processed to determine their dependence on the frequency and the time variation of the signal amplitude.

The phase transitions in ^3He in aerogel were manifested by changes in the frequency, amplitude, and duration of the free induction signal in response to application of the small RF signals (corresponding to

the angles of magnetization rotation below $\sim 20^\circ$). Upon cooling below the superfluid transition temperature of ^3He in aerogel ($T_c^a \approx 0.76 T_c$, where $T_c = 2.37$ mK is the superfluid transition temperature for bulk ^3He under the given conditions), the system exhibited two sequential transitions. First, there appeared and increased a negative shift of the NMR frequency relative to the Larmor value, which was related to the transition to a supercooled ^3He A-like phase in aerogel. Then, at a certain temperature about $\approx 0.85 T_c^a$, the sample converted into a B-like phase whereby the frequency shift became positive and increased with further decrease in the temperature [10]. On heating from the B-like phase, the shift decrease in proportion to $(1 - T/T_c^a)$ and vanished (being always positive) at $T = T_c^a$. These results agree with the recent experiments [4] where a similar behavior was observed by a continuous NMR technique.

It was established that the free induction signal at large magnetization rotation angles significantly varies with time. For determining the dependence of ω on β , the time variation of the induction signal was extrapolated to the initial time instant (it should be noted that the results remain qualitatively the same for any reasonable method of determining the characteristic frequency at a given β , for example, by taking the average frequency of the Fourier transform of the induction signal). Figure 2 shows a plot of the induction signal frequency versus initial magnetization rotation angle for ^3He B-like phase in aerogel. As can be seen, the experimental curves exhibit a feature at $\beta \approx 104^\circ$ whereby the signal frequency begins to grow sharply with β , as it should be expected for the B-phase. At the same time, we observed no signs of a texture transition to the Brinkman–Smith precession mode. As can be seen, the precession frequency at any magnetization rotation angle below 104° is significantly shifted from the Larmor value, while still varies depending on β . This result indicates that texture of the order parameter is determined by the aerogel volume (and, probably, by the aerogel density inhomogeneities over distances much shorter than the characteristic cell size), rather than by walls of the experimental cell.

5. HPD of ^3He -B in aerogel. Experiments devoted to determining the possibility of the HPD formation in aerogel were performed with both cells. Figure 3 shows the continuous NMR signal profiles measured in cell 1 on decreasing H_0 for various RF field amplitudes. The abscissa axis in Fig. 3 (and in the other plots of continuous NMR signals) shows the homogeneous component of the applied magnetic field recalculated into a coordinate by the formula $z = (\gamma H - \omega_{rf})/\gamma \sqrt{H}$. The point $z = 0$ corresponds to validity of the resonance condition for bulk ^3He at the cell top, and $z = -5.6$, at the cell bottom. When the domain wall occurs inside the cell, the resonance condition is obeyed at the middle of the wall

(this is true for bulk ^3He -B and will be shown below to hold for an HPD in aerogel as well), and the abscissa in fact indicates the domain wall position.

As can be seen, the signal observed for a pumping field amplitude of ~ 0.02 Oe (Fig. 3b) is significantly higher than the signals measured at smaller amplitudes of pumping, which corresponds to the HPD formation, growth (whereby the HPD occupies the entire cell), and breakage (for $z \approx -9.4$ mm). Upon breakage, no HPD is formed during the reverse scan. Our calibration of the NMR spectrometer showed that the NMR signal amplitude (Fig. 3b) corresponds to within 10% to an amplitude of the NMR signal anticipated from the HPD.

Figure 4 shows variation of the induction signal amplitude and frequency with time after the HPD was "grown" as described above and the RF field was switched off. As can be seen, the signal amplitude exhibits oscillations (rather than smoothly decays to zero as in the case of bulk ^3He [7]), although the characteristic signal duration is large and the frequency kinetics on the average well agrees with that expected for a slow relaxation of the HPD. A complete change of the induction signal frequency amounts to ~ 1590 Hz, which coincides to a good accuracy with the frequency change calculated by the formula $\delta\omega = \gamma\nabla H L_0$ (where L_0 is the HPD length immediately before switching off the RF field), as it has to be in the case of the HPD formation. Oscillations of the induction signal amplitude may be caused by spatial inhomogeneities (or anisotropy) of the aerogel density. These would result in inhomogeneities within the HPD and in a nonuniform magnetic dissipation over the HPD volume. This would lead to inhomogeneous β distribution over the sample and to dephasing of the precession in various parts of the aerogel. Spin supercurrents will tend to restore the homogeneous precession, thus giving rise oscillations in the precession phase distribution, analogous to the torsional HPD oscillations observed in bulk ^3He -B [11].

It should be noted that the magnetic dissipation may give rise, due to a low thermal conductivity of ^3He in aerogel, to significant temperature nonuniformities and the resulting HPD inhomogeneities. In our experiments with continuous NMR, the HPD formation in cell 1 as accompanied by an increase in the temperature of ^3He in aerogel because of the magnetic relaxation leading to the energy dissipation. When the H_0 variation was stopped (i.e., the HPD length was fixed), the sample temperature continued to grow at a time constant on the order of one minute (estimates obtained from the data [12] on the thermal conductivity of ^3He in aerogel show that overheating may reach up to $0.1\text{--}0.2T_c^a$ at a characteristic power of several nanowatts dissipated in aerogel). The magnetic relaxation rate increases with the temperature and the HPD breaks within several minutes, since the dissipated power exceeds a maximum possible value of the absorbed power at a given RF field amplitude.

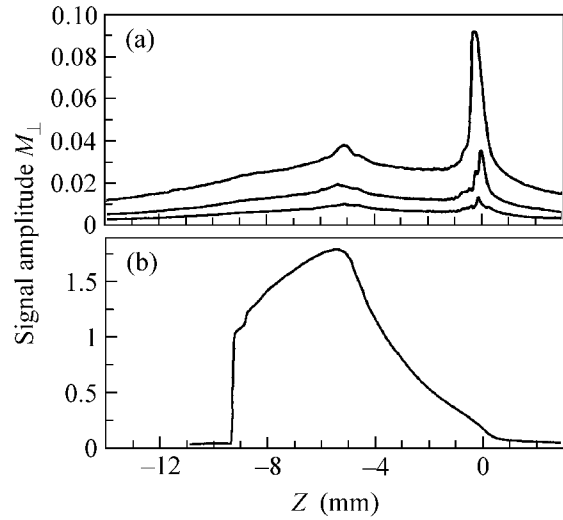


Fig. 3. Transverse magnetization amplitude profiles (M is the square root of the sum of squared absorption and dispersion signal intensities) measured at $\nabla H = 284$ Oe, $H = 1$ Oe/cm, $T \sim 0.67T_c^a$ and various RF field amplitudes: (a) 0.002, 0.005, and 0.01 Oe, in the order of increasing average signal intensity; (b) 0.02 Oe.

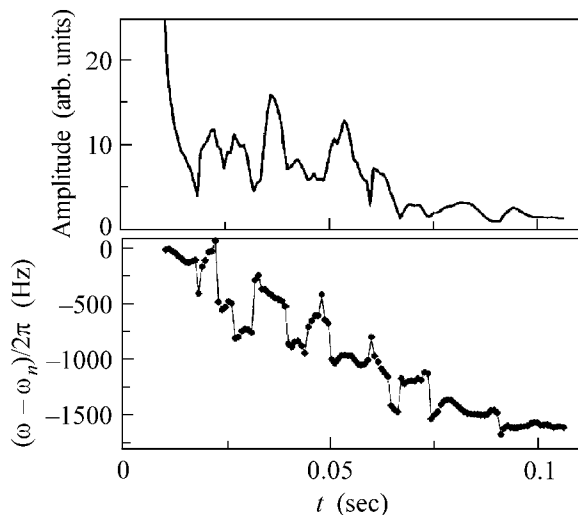


Fig. 4. Time variation of the amplitude and frequency of a long-lived NMR induction signal after switching off the RF field at an HPD length of ~ 4.9 mm in cell 1. The experimental conditions are the same as indicated for Fig. 3b.

The overheating effects were virtually not manifested in cell 2, where a maximum distance from the aerogel center to bulk ^3He was several times smaller than in cell 1. In cell 2, the HPD initially formed, as a rule, in the volume free of aerogel. As the HPD length increased, it penetrated into aerogel and eventually filled the entire cell. Figure 5 shows the absorption and dispersion profiles measured during the HPD formation

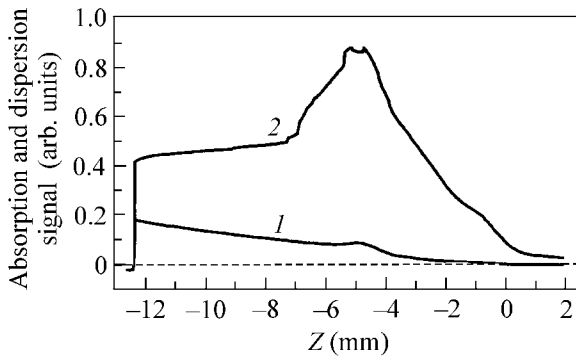


Fig. 5. Profiles of the (1) NMR absorption and (2) dispersion signals during the HPD formation in cell 2 for $H = 284$ Oe, $\nabla H = 0.94$ Oe/cm, $T \sim 0.67 T_c^a$, an RF field amplitude of ~ 0.01 Oe.

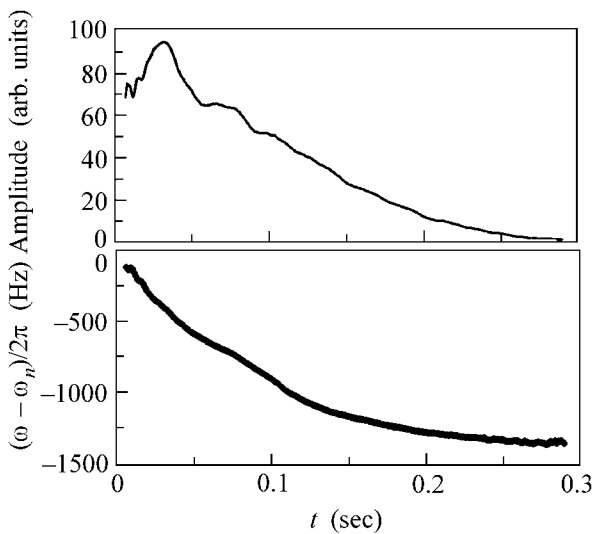


Fig. 6. Time variation of the amplitude and frequency of a long-lived NMR induction signal after switching off the RF field at an HPD length of ~ 4.7 mm in cell 3. The experimental conditions are the same as indicated for Fig. 5.

in cell 2. Here (as well as in Fig. 3) the value $z = 0$ on the abscissa axis corresponds to validity of the resonance condition for bulk ^3He at the cell top, the value of $z = -5.6$ implies the same at the cell bottom, while $z = -1.5$ and -3.9 mm correspond to the aerogel–bulk ^3He boundaries.

As can be seen from Fig. 5, the NMR absorption both in bulk ^3He and in aerogel monotonically increases with the HPD length (a faster signal buildup in the initial HPD growth stage is related to the domain wall formation). Note that no sharp features are observed when the domain wall crosses the aerogel–bulk ^3He interface. Previously, we repeatedly observed the growth of the HPD absorption by a nearly linear law

(over the HPD length) for bulk ^3He (unpublished data of many experiments performed in the past years). A mechanism of this absorption still remains unclear and requires further investigation. Here, we will only note that this mechanism is effective in aerogel as well. It was found (in this study, as well as in the preceding experiments with bulk ^3He) that the absorption increases with the temperature and is virtually independent of the external magnetic field gradient.

In contrast to the results of experiments in cell 1, the amplitude and frequency of the induction signal from the HPD, measured after switching off the RF field, varied in a smooth manner, which was indicative of a homogeneity of the HPD retained in the course of the relaxation process (Fig. 6). No distinguishable features were observed at a frequency of the induction signal corresponding to a moment of the domain wall crossing the aerogel–bulk ^3He boundary (for a current coordinate determined by the signal frequency).

Using the sample in cell 2, we have also studied the temperature dependence of the HPD formation process. It was established that the HPD did not penetrate into aerogel at a temperature slightly below T_c^a (usually, on the order of $0.9 T_c^a$), although an HPD in the upper aerogel-free volume part of the cell forms even at temperatures up to that corresponding to the transition of bulk ^3He into the A phase ($T_{AB} \approx 1.2 T_c^a$). On the other hand, an inverse pattern was observed at a sufficiently low temperature: the HPD formation in the volume (aerogel-free) part of cell 2 took place at a greater RF field amplitudes as compared to those in aerogel. As a result, there was a certain interval of the RF field amplitudes in which it was possible to form an HPD only in aerogel in the absence of HPD in bulk ^3He .

Figure 7 shows two NMR signal profiles measured at $T \approx 0.65 T_c^a$ for different amplitudes of the RF field (curve 2 corresponds to the case of the HPD formation in aerogel only). The fact that the abscissa corresponding to the signal growth onset (curve 2) is close to the coordinate of the aerogel–bulk ^3He interface shows that the NMR frequency in the domain wall is close to the Larmor value; this is probably indicative of a texture transition of the Brinkman–Smith type in the case of the HPD formation in aerogel under the continuous NMR conditions. In contrast to the pulsed NMR data (Fig. 2), this results in an almost zero shift of the precession frequency from the Larmor value at the magnetization rotation angles close to Θ_0 (otherwise, the HPD signal growth onset would be shifted to the left by a value corresponding to the frequency shift from the Larmor value, which amounts to not less than 1 mm in the z scale).

6. Conclusion. The results of our investigation leave no doubts that a low-temperature superfluid ^3He phase in aerogel is analogous to the B phase of bulk ^3He . It

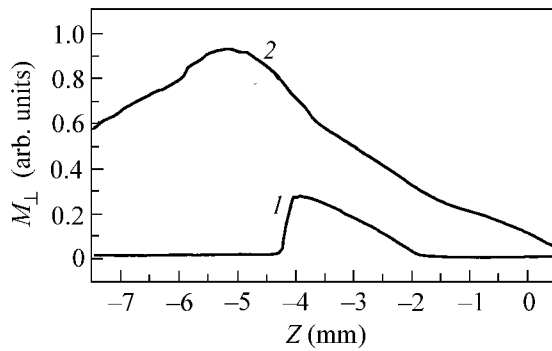


Fig. 7. Transverse magnetization amplitude profiles (M is the square root of the sum of squared absorption and dispersion signal intensities) measured at $H = 284$ Oe, $\nabla H = 0.94$ Oe/cm, $T \approx 0.65 T_c^a$ and an RF field amplitude of (1) 0.02 Oe and (2) 0.04 Oe.

was demonstrated that an important role in the spin dynamics of ^3He B-like phase in aerogel, as well as in bulk ^3He -B, belongs to the spin supercurrents which can lead to the formation of a homogeneous precession domain. Similar to the case of bulk ^3He -B, the HPD formation can be used as a probe for studying the superfluid ^3He -B phase in aerogel. In particular, it would be very interesting to elucidate questions concerning the observation and study of the “catastrophic” relaxation of ^3He in aerogel, by analogy with the phenomenon taking place in bulk ^3He -B at temperatures on the order of $0.4 T_c$ [13], the nature of which is still unclear.

The authors are grateful to J. Parpia for kindly providing the cell partly filled with aerogel for the experiments, and to I. Fomin for fruitful discussions.

This study was supported by the U.S. Civilian Research and Development Foundation (grant no. RP1-2098), by the Russian Foundation for Basic Research (project nos. 00-02-17514 and 00-15-96574), and by the Ministry of Industry, Science, and Technology of the Russian Federation.

SPELL: precessing, bu

REFERENCES

1. J. V. Porto and J. M. Parpia, *Phys. Rev. Lett.* **74**, 4667 (1995).
2. D. T. Sprague, T. M. Haard, J. B. Kycia, *et al.*, *Phys. Rev. Lett.* **75**, 661 (1995).
3. G. Gervais, T. M. Haard, R. Nomura, *et al.*, *Phys. Rev. Lett.* **87**, 035701 (2001).
4. B. I. Barker, Y. Lee, L. Polukhina, *et al.*, *Phys. Rev. Lett.* **85**, 2148 (2000).
5. A. S. Borovik-Romanov, Yu. M. Bun'kov, V. V. Dmitriev, and Yu. M. Mukharskiĭ, *Pis'ma Zh. Éksp. Teor. Fiz.* **37**, 600 (1983) [*JETP Lett.* **37**, 716 (1983)]; V. L. Golo, A. A. Leman, and I. A. Fomin, *Pis'ma Zh. Éksp. Teor. Fiz.* **38**, 123 (1983) [*JETP Lett.* **38**, 146 (1983)].
6. A. S. Borovik-Romanov, Yu. M. Bun'kov, V. V. Dmitriev, *et al.*, *Zh. Éksp. Teor. Fiz.* **88**, 2025 (1985) [*Sov. Phys. JETP* **61**, 1199 (1985)]; I. A. Fomin, *Zh. Éksp. Teor. Fiz.* **88**, 2039 (1985) [*Sov. Phys. JETP* **61**, 1207 (1985)].
7. A. S. Borovik-Romanov, Yu. M. Bun'kov, V. V. Dmitriev, *et al.*, *Zh. Éksp. Teor. Fiz.* **96**, 956 (1989) [*Sov. Phys. JETP* **69**, 542 (1989)].
8. D. T. Sprague, T. M. Haard, J. B. Kycia, *et al.*, *Phys. Rev. Lett.* **77**, 4568 (1996).
9. Yu. M. Bun'kov, in *Proceedings of Seminar of the Institute of Physical Problems, Russian Academy of Sciences, 2001*; Yu. Bunkov, E. Collin, H. Godfrin, and R. Harakaly, in *Proceedings of 23rd International Conference on Low Temperature Physics, LT23, Hiroshima, 2002*, submitted to *Physica B*.
10. V. V. Dmitriev, I. V. Kosarev, N. Mulders, *et al.*, in *Proceedings of 23rd International Conference on Low Temperature Physics, LT23, Hiroshima, 2002*, submitted to *Physica B*.
11. Yu. M. Bun'kov, V. V. Dmitriev, and Yu. M. Mukharskiĭ, *Pis'ma Zh. Éksp. Teor. Fiz.* **43**, 131 (1986) [*JETP Lett.* **43**, 168 (1986)]; I. A. Fomin, *Pis'ma Zh. Éksp. Teor. Fiz.* **43**, 134 (1986) [*JETP Lett.* **43**, 171 (1986)].
12. B. I. Barker, L. Polukhina, J. F. Poko, *et al.*, *J. Low Temp. Phys.* **113**, 635 (1998).
13. Yu. M. Bunkov, V. V. Dmitriev, J. Nyeki, *et al.*, *Physica B (Amsterdam)* **165-166**, 675 (1990); Yu. M. Bunkov, S. N. Fisher, A. M. Guenault, *et al.*, *Phys. Rev. Lett.* **68**, 600 (1992).

Translated by P. Pozdeev